Inorganic Chemistry

Article

Structural Analysis, Spectroscopic, and Magnetic Properties of the 1D Triple-Bridged Compounds [M(dca)$_2$(bpa)] (M = Mn, Fe, Co, Zn; dca = dicyanamide; bpa = 1,2-bis(4-pyridyl)ethane) and the 3D [Ni(dca)(bpa)$_2$]dca · 6H$_2$O

Noelia de la Pinta,[†] Susana Martín,[⊥,#] M. Karmele Urtiaga,[‡] M. Gotzone Barandika,[⊥] M. Isabel Arriortua,[‡] Luis Lezama,[†] Gotzon Madariaga,[§] and Roberto Cortés*[,†]

[†]*Departamento de Química Inorgánica,* [‡]*Departamento de Mineralogía y Petrología, and*
[§]*Departamento de Física de la Materia Condensada, Facultad de Ciencia y Tecnología,*
Universidad del País Vasco, Aptdo. 644, 48080 Bilbao, Spain, and [⊥]*Departamento de Química Inorgánica,*
Facultad de Farmacia, Universidad del País Vasco, Aptdo. 450, 01080 Vitoria-Gasteiz, Spain.
[#]*Current address: Departamento de Biotecnología, Universidad Francisco de Vitoria,*
Ctra Pozuelo-Majadahonda km 1, 800, 28223 Pozuelo de Alarcón (*Madrid*), *Spain.*

The family of compounds [Mn(dca)$_2$(bpa)] (**1**), [Fe(dca)$_2$(bpa)] (**2**), [Co(dca)$_2$(bpa)] (**3**), [Zn(dca)$_2$(bpa)] (**4**), and [Ni(dca)(bpa)$_2$]dca · 6H$_2$O (**5**), with dca = dicyanamide and bpa = 1,2-bis(4-pyridyl)ethane, has been synthesized. These compounds have been characterized by single crystal (**1**, **2**, **4**, and **5**) and powder X-ray diffraction (**3**), by Fourier transform infrared (FTIR), UV–vis, and electron paramagnetic resonance (EPR) spectroscopies, and by magnetic measurements. Compound **1** crystallizes in the monoclinic $C2/c$ space group, $Z = 4$, with $a = 16.757(6)$, $b = 9.692(3)$, and $c = 13.073(4)$ Å, and $\beta = 123.02(2)°$; Compound **2** crystallizes in the monoclinic $C2/c$ space group, $Z = 4$, with $a = 16.588(5)$, $b = 9.661(3)$, $c = 12.970(5)$ Å, and $\beta = 123.16(3)°$; Compound **4** crystallizes in the monoclinic $C2/c$ space group, $Z = 4$, with $a = 16.519(2)$, $b = 9.643(2)$, $c = 12.943(2)$ Å, and $\beta = 123.15(1)°$; Compound **5** crystallizes in the monoclinic $C2/c$ space group, $Z = 4$, with $a = 18.504(4)$, $b = 19.802(3)$, and $c = 8.6570(18)$ Å, and $\beta = 99.74(2)°$. The compounds **1**–**4** are isostructural and show a one dimensional (1D) disposition, with the metal(II) ions bridged by double $\mu_{1,5}$ dca ligands and unusually by a third bridge consisting of the bpa ligand, which adopts a very low torsion angle to accommodate in the structure. This kind of structure is unusual, even considering the voluminous bpa bridge. The compound **5** shows a 3D structure with layers of Ni-bpa joined by single dca bridges. Magnetic susceptibility measurements show antiferromagnetic couplings, increasing for **1**–**3**. Compound **5** shows very slight antiferromagnetic interactions.

Introduction

A considerable ongoing research has been directed, over the last decade, at the design and preparation of coordination metal complexes with multidimensional network structures because of their fascinating physical properties, potential applications, and the aesthetic beauty and complexity of their structures. Thus, the preparation of crystalline materials exhibiting some desired structural and topological features becomes a fascinating challenge as it implies the control on the related physical and chemical properties. In this sense, the strategy of synthesis has been widely confirmed to be a determinant factor.

Among the variety of extended frameworks reported during the past years, there are plenty of examples that could illustrate the relevance of the synthesis strategy. Since the azide pseudohalide has been one of the most used ligands,[1] it has been observed that the lower is the number of coordinating atoms of the organic blocking ligand, from the tridentate terpyridine to 4,4′-bipy-type ones, the larger is the dimensionality of the formed system.[2,3]

*Corresponding author. E-mail: roberto.cortes@ehu.es.
(1) (a) Pierpont, C. G.; Hendrickson, D. N.; Duggan, D. M.; Wagner, F.; Barefield, E. K. *Inorg. Chem.* **1975,** *14,* 604–610. (b) Commarmond, J.; Plumere, P.; Lehn, J. M.; Agnus, Y.; Louis, R.; Weiss, R.; Kahn, O.; Morgenstern-Badarau, I. *J. Am. Chem. Soc.* **1982,** *104,* 6330–6340. (c) Ribas, J.; Monfort, M.; Vicente, R.; Escuer, A.; Cortés, R.; Lezama, L; Rojo, T. *Coord. Chem. Rev.* **1999,** *193–195,* 1027–1068 and references therein; (d) Escuer, A.; Aromí, G. R. *Eur. J. Inorg. Chem.* **2006,** 4721–4736 and references therein.

(2) (a) Cortés, R.; Pizarro, J. L.; Lezama, L.; Arriortua, M. I.; Rojo, T. *Inorg. Chem.* **1994,** *33,* 2697–2700. (b) Cortés, R.; Drillon, M.; Solans, X.; Lezama, L; Rojo, T. *Inorg. Chem.* **1997,** *36,* 677–683.

(3) (a) Cortés, R.; Lezama, L.; Pizarro, J. L.; Arriortua, M. I.; Rojo, T. *Angew. Chem., Int. Ed. Engl.* **1996,** *35,* 1810–1812. (b) Cortés, R.; Urtiaga, M. K.; Lezama, L.; Pizarro, J. L.; Arriortua, M. I; Rojo, T. *Inorg. Chem.* **1997,** *36,* 5016–5021. (c) Hernandez, M. L.; Barandika, M. G.; Urtiaga, M. K.; Cortés, R.; Lezama, L.; Arriortua, M. I.; Rojo, T. *J. Chem. Soc., Dalton Trans.* **1999,** 1401–1406.
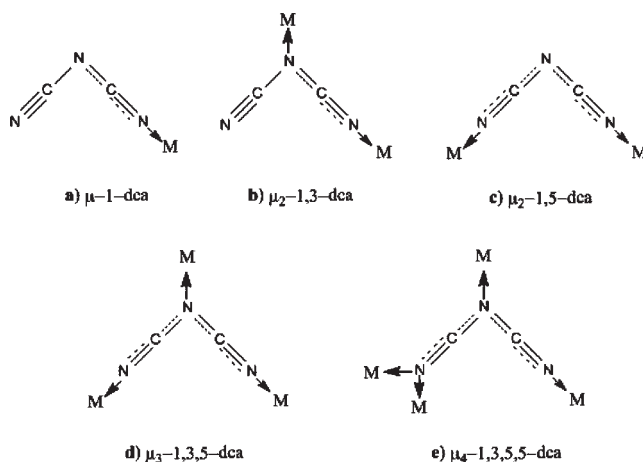
In fact, over the past decade a great amount of coordination networks exhibiting 4,4′dipyridyl-type ligands have been reported.[4] Among them, bpa is characterized by a remarkable high capability to get accommodated in the structural

Scheme 1. Coordination Modes of Dca

a) μ−1−dca b) μ₂−1,3−dca c) μ₂−1,5−dca

d) μ₃−1,3,5−dca e) μ₄−1,3,5,5−dca

framework. Thus, as a consequence of the freedom of rotation exhibited by the ethane group, bpa can adopt two different conformations, anti and gauche, both conformers being able to perform as coordinating ligands (either bridging or terminal) and/or as templates by crystallizing in the cavities of the cell. This flexibility makes bpa an excellent candidate for the preparation of coordination polymers, as illustrated by the increasing number of bpa polymers reported during the past decade.[5]

In this context, a further step on the synthesis strategy could consist of the substitution of the azide group by

(4) (a) Robson, I. R.; Abrahams, B. F.; Batten, S. R.; Gable, R. W.; Hoskins, B. F.; Liu, J. *Supramolecular Arquitecture*; American Chemical Society: Washington, DC, 1992; (b) Dossier, P.; Zaworotko, M. J. *Angew. Chem., Int. Ed. Engl.* **1996**, *35*, 2779. (c) Hagrman, D.; Hammond, R. P.; Haushalter, R.; Zubieta, J. *Chem. Mater.* **1998**, *10*, 2091. (d) Kondo, M.; Yoshitomi, T.; Seki, K.; Matzusaka, H.; Kitagawa, S. *Angew. Chem., Int. Ed. Engl.* **1997**, *36*, 1725. (e) Real, J. A.; Andrés, E.; Muñoz, M. C.; Julve, M.; Granier, A.; Bousseksou, A.; Varret, F. *Science* **1995**, *268*, 265–268. (f) Shi, Z.; Feng, S.; Gao, S.; Zhang, L.; Yang, G.; Hua, J. *Angew. Chem., Int. Ed. Engl.* **2000**, *39*, 2325–2327. (g) Sun, H.-L.; Gao, A.; Ma, B.-Q.; Batten, S. R. *Cryst. Eng. Comm.* **2004**, 579–583. (h) Konar, S.; Manna, S. C.; Zangrando., E.; Mallah, T.; Ribas, J.; Chaudhuri, N. R. *Eur. J. Inorg. Chem.* **2004**, 4202–4208. (i) Zang, S. Q.; Su, Y.; Li, Y. Z.; Zhu, H. Z.; Meng, Q. J. *Inorg. Chem.* **2006**, *45*, 2972–2978. (j) Liang, S.; Liu, Z.; Liu, C.; Di, X.; Zhang, D. Z. *Anorg. Allg. Chem.* **2009**, *635*, 549–553. (k) Ma, L.-F.; Wang, L.-Y.; Du, M.; Batten, S. R. *Inorg. Chem.* **2010**, *49*, 365–367.

(5) (a) Hennigar, T. L.; MacQuarrie, D. C.; Losier, P.; Rogers, R. D.; Zaworotko, M. J. *Angew. Chem., Int. Ed. Engl.* **1997**, *36*, 972–74. (b) Power, K. N.; Hennigar, T. L.; Zaworotko, M. J. *Chem. Commun.* **1998**, 595–597. (c) Hong, C. S.; Son, S.-K.; Lee, Y. S.; Jun, M.-J.; Do, Y. *Inorg. Chem.* **1999**, *38*, 5602. (d) Carlucci, L.; Ciani, G.; Proserpio, D. M.; Rizzato, S. *Chem. Commun.* **2000**, 1319. (e) Hernandez, M. L.; Barandika, M. G.; Urtiaga, M. K.; Cortés, R.; Lezama, L.; Arriortua, M. I. *J. Chem. Soc., Dalton Trans.* **2000**, 79–84. (f) Hernandez, M. L.; Urtiaga, M. K.; Barandika, M. G.; Cortés, R.; Lezama, L.; De la Pinta, N.; Arriortua, M. I.; Rojo, T. *J. Chem. Soc., Dalton Trans.* **2001**, 3010–3014. (g) Carranza, J.; Brennan, C.; Sletten, J.; Lloret, F.; Julve, M. *J. Chem. Soc., Dalton Trans.* **2002**, 3164–3170. (h) Jude, H.; Krause Bauer, J. A.; Connig, W. B. *Inorg. Chem.* **2005**, *44*, 1211–1220. (i) Lima, P. P.; Almeida Paz, F. A.; Ferreira, R. A. S.; Bermúdez, V. Z.; Carlos, L. D. *Chem. Mater.* **2009**, *21*, 5099–5111. (j) Ma, L.-F; Liu, B.; Wang, L.-Y.; Li, C.-P.; Du, M. *Dalton Trans.* **2010**, *39*, 2301–2308.

(6) (a) Potocnák, I.; Dunaj-Jurco, M.; Miklos, D.; Kabesová, M. *Acta Crystallogr.* **1995**, *C51*, 600–602. (b) Potocnák, I.; Dunaj-Jurco, M.; Miklos, D. M; Jäger, A. *Acta Crystallogr.* **1996**, *C52*, 1653–1655. (c) Miyasaka, H.; Nakata, K.; Lecren, L.; Coulon, C.; Nakazawa, Y.; Fujisaki, T.; Sugiura, K.; Yamashita, M.; Clerac, R. *J. Am. Chem. Soc.* **2006**, *128*, 3770–3783. (d) Zhao, X.-J.; Wang, Q.; Du, M. *Inorg. Chim. Acta* **2007**, *360*, 1970–1976. (e) Youngme, S.; Chotkhun, T.; Chaichit, N.; Van Albada, G. A.; Reedijk, J. *Inorg. Chem. Commun.* **2007**, *10*, 843–848. (f) Costa, J. S.; Lappalainen, K.; de Ruiter, G.; Quesada, M.; Tang, J.; Mutikainen, I.; Turpeinen, U.; Grunert, C. M.; Gutlich, P.; Lazar, H. Z.; Letard, J.-F.; Gamez, P.; Reedijk, J. *Inorg. Chem.* **2007**, *46*, 4079–4089. (g) Ge, H.; Liu, K.; Rang, Y.; Li, B.; Zhang, Y. *Inorg. Chem. Commun.* **2008**, *11*, 260–264. (h) Liu, K.; Zhang, Y.-M.; Yang, Y.; Li, B.-L.; Zhang, Y. *J. Coord. Chem.* **2008**, *61*, 2926–2934. (i) Sheu, C.-F.; Pillet, S.; Lin, Y.-C.; Chen, S.-M.; Hsu, I.-J.; Lecomte, C.; Wang, Y. *Inorg. Chem.* **2008**, *47*, 10866–10874. (j) Callejo, L.; De La Pinta, N.; Vitoria, P.; Cortés, R. *Acta Crystallogr.* **2009**, *E65*, m68–m69. (k) Honzicek, J.; Vinklarek, J.; Cisarova, I.; Erben, M. *Inorg. Chim. Acta* **2009**, *362*, 83–88.

(7) (a) Chow, Y. M. *Inorg. Chem.* **1971**, *10*, 1938–1942. (b) Chow, Y. M.; Britton, D. *Acta Crystallogr.* **1977**, *C33*, 697. (c) Britton, D. *Acta Crystallogr.* **1990**, *C46*, 2297–2299. (d) Manson, J. L.; Incarvito, C. D.; Rheinhold, A. L; Miller, J. S. *J. Chem. Soc., Dalton Trans.* **1998**, 3705–3706. (e) Mrozinski, J.; Hvastijová, M.; Kohout, J. *Polyhedron* **1992**, *11*, 2867–2871. (f) Martin, S.; Barandika, M. G.; R. de Larramendi, J. I.; Cortés, R.; Font-Bardía, M.; Lezama, L.; Serna, Z. E.; Solans, X.; Rojo, T. *Inorg. Chem.* **2001**, *40*, 3687–3692. (g) Martin, S.; Barandika, M. G.; Cortés, R.; R. de Larramendi, J. I.; Urtiaga, M. K.; Lezama, L.; Arriortua, M. I.; Rojo, T. *Eur. J. Inorg. Chem.* **2001**, 2107–2112. (h) Martin, S.; Barandika, M. G.; Ezpeleta, J. M.; Cortés, R.; R. de Larramendi, J. I.; Lezama, L.; Rojo, T. *J. Chem. Soc., Daton. Trans.* **2002**, 4275–4280. (i) Zhu, L.-N.; Xu, N.; Zhang, W.; Liao, D.-Z.; Yoshimura, K.; Mibu, K.; Jiang, Z.-H.; Yang, S.-P.; Cheng, P. *Inorg. Chem.* **2007**, *46*, 1297–1304. (j) Mason, J. L.; Schlueter, J. A.; Nygren, C. L. *Dalton Trans.* **2007**, 646–652. (k) Gu, Z.-G.; Zhou, X.-H.; Jin, Y.-B.; Xiong, R.-G.; Zuo, J.-L.; You, X.-Z. *Inorg. Chem.* **2007**, *46*, 5462–5464. (l) Suarez-Varela, J.; Mota, A. J.; Aouryaghal, H.; Cano, J.; Rodriguez-Dieguez, A.; Luneau, D.; Colacio, E. *Inorg. Chem.* **2008**, *47*, 8143–8158. (m) Mal, D.; Sen, R.; Adhikary, C.; Miyashita, Y.; Okamoto, K.-I.; Bhattacharjee, A.; Gutlich, P.; Koner, S. *J. Coord. Chem.* **2008**, *61*, 3486–3492. (n) Gomez-Saiz, P.; Gil-Garcia, A.; Maestro, M. A.; Arnaiz, F. J.; Lezama, L.; Rojo, T.; Pizarro, J. L.; Arriortua, M. I.; Gonzalez-Alvarez, M.; Borras, J.; Diez-Gomez, V.; Garcia-Tojal, J. *Eur. J. Inorg. Chem.* **2009**, 373–388. (o) Wang, S.; Wang, L.; Li, B.; Zhang, Y. *J. Chem. Cryst.* **2009**, *39*, 221–224. (p) Du, M.; Zhang, Z.-H.; Wang, X.-G.; Zhao, X.-J. *Inorg. Chim. Acta* **2009**, *362*, 1358–1360.

(8) (a) Manson, J. L.; Kmety, C. R.; Huang, Q.; Lynn, J. W.; Bendele, G.; Pagola, S.; Stephens, P. W.; Liable-Sands, L. M.; Rheingold, A. L.; Epstein, A. J.; Miller, J. S. *Chem. Mater.* **1998**, *10*, 2552–2560. (b) Ding, B.; Li, J.; Yang, E.-C.; Wang, X.-G.; Zhao, X.-J. *Z. Anorg. Allg. Chem.* **2007**, *633*, 1062–1065.

(9) (a) Chow, Y. M.; Britton, D. *Acta Crystallogr.* **1975**, *C31*, 1934–1937. (b) Jurgens, B.; Hoppe, H. A.; Schnick, W. *Solid State Sci.* **2002**, *4*, 821–825. (c) Shi, Y.-J.; Chen, X.-T.; Li, Y.-Z.; Xue, Z.; You, X.-Z. *New J. Chem.* **2002**, *26*, 1711–1713.

(10) (a) Batten, S. R.; Jensen, P.; Moubaraki, B.; Murray, K. S.; Robson, R. *Chem. Commun.* **1998**, 439–440. (b) Manson, J. L.; Lee, D. W.; Rheingold, A. L.; Miller, J. S. *Inorg. Chem.* **1998**, *37*, 5966–5967. (c) Manson, J. L.; Kmety, C. R.; Epstein, A. J.; Miller, J. S. *Inorg. Chem.* **1999**, *38*, 2552–2553. (d) Jensen, P.; Batten, S. R.; Fallon, G. D.; Moubaraki, B.; Murray, K. S.; Price, D. J. *Chem. Commun.* **1999**, 177–178. (e) Batten, S. R.; Jensen, P.; Kepert, C. J.; Kurmoo, M.; Moubaraki, B.; Murray, K. S.; Price, D. J. *J. Chem. Soc., Dalton Trans.* **1999**, 2987–2297. (f) Jensen, P.; Batten, S. R.; Fallon, G. D.; Hockless, D. C. R.; Moubaraki, B.; Murray, K. S.; Robson, R. *J. Solid State Chem.* **1999**, *145*, 387–393. (g) Manson, J. L.; Arif, A. M.; Miller, J. S. *J. Mat. Chem.* **1999**, *9*, 979–983. (h) Jensen, P.; Batten, S. R.; Moubaraki, B.; Murray, K. S. *Chem. Commun.* **2000**, 793–794. (i) Marshall, S. R.; Incarvito, C. D.; Manson, J. L.; Rheingold, A. L.; Miller, J. S. *Inorg. Chem.* **2000**, *39*, 1969–1973. (j) Sun, B.-W.; Gao, S.; Ma, B.-Q.; Wang, Z.-M. *Inorg. Chem. Commun.* **2001**, *4*, 72–75. (k) Vangdal, B.; Carranza, J.; Lloret, F.; Julve, M.; Sletten, J. *J. Chem. Soc., Dalton Trans.* **2002**, 566–574. (l) Marshall, S. R.; Rheingold, A. L.; Dawe, L. N.; Shum, W. W.; Kitamura, C.; Miller, J. S. *Inorg. Chem.* **2002**, *41*, 3599–3601. (m) Manson, J. L.; Gu, J.; Schlueter, J. A.; Wang, H.-H. *Inorg. Chem.* **2003**, *42*, 3950–3955. (n) Miyasaka, H.; Nakata, K.; Sigiura, K.; Yamashita, M.; Clerac, R. *Angew. Chem., Int. Ed.* **2004**, *43*, 707–711. (o) Colacio, E.; Maimoun, I. B.; Lloret, F.; Suarez-Varela, J. *Inorg. Chem.* **2005**, *44*, 3771–3773. (p) Can Albada, G. A.; Mutikainen, I.; Turpeinen, U.; Reedijk, J. *Inorg. Chem. Comun.* **2006**, *9*, 441–443. (q) Ding, N.-N.; Zhang, W.-H.; Li, H.-X.; Ren, Z.-G.; Lang, J.-P.; Zhang, Y.; Abrahams, B. F. *Inorg. Chem. Commun.* **2007**, *10*, 623–626. (r) Gu, Z.-G.; Zhou, X.-H.; Jin, Y.-B.; Xiong, R.-G.; Zuo, J.-L.; You, X.-Z. *Inorg. Chem.* **2007**, *46*, 5462–5464. (s) Kushch, N. D.; Yagubskii, E. B.; Kartsovnik, M. V.; Buravov, L. I.; Dubrovski, A. D.; Chekhlov, A. N.; Biberacher, W. *J. Am. Chem. Soc.* **2008**, *130*, 7238–7240. (t) Branzea, D. G.; Sorace, L.; Maxim, C.; Andruh, M.; Caneschi, A. *Inorg. Chem.* **2008**, *47*, 6590–6592. (u) Ray, A.; Pilet, G.; Gomez-Garcia, C. J.; Mitra, S. *Polyhedron* **2009**, *28*, 511–520. (v) Kushch, N. D.; Kazakova, A. V.; Buravov, L. I.; Chekhlov, A. N.; Dubrovskii, A. D.; Yagubskii, E. B.; Canadell, E. *J. Solid State Chem.* **2009**, *182*, 617–621.

Table 1. Crystallographic Collection and Refinement Parameters for Compounds **1**, **2**, **4**, and **5**

	Mn (**1**)	Fe (**2**)	Zn (**4**)	Ni (**5**)
formula	$MnC_{16}H_{12}N_8$	$FeC_{16}H_{12}N_8$	$ZnC_{16}H_{12}N_8$	$NiC_{28}H_{36}N_{10}O_6$
M_r	371.28	372.19	381.71	667.38
cryst. syst.	monoclinic	monoclinic	monoclinic	monoclinic
space group	$C2/c$	$C2/c$	$C2/c$	$C2/c$
a [Å]	16.757(6)	16.588(5)	16.519(2)	18.504(4)
b [Å]	9.692(3)	9.661(3)	9.643(2)	19.802(3)
c [Å]	13.073(4)	12.970(5)	12.943(2)	8.6570(18)
β [°]	123.02(2)	123.16(3)	123.15(1)	99.74(2)
V [Å³]	1780.2(10)	1739.9(9)	1726.1(4)	3126.3(11)
Z	4	4	4	4
$F(000)$	756	760	776	1400
ρ_{caled} [g cm⁻³]	1.385	1.421	1.469	1.418
μ(Mo K_α)/mm⁻¹	0.757	0.882	1.439	0.679
range [°]	2.65−25.77	2.57−25.87	2.57−29.99	2.06−26.0
reflns coled	5514	6560	5159	12153
indep reflns	1609	1636	2523	3030
parameters	134	115	134	232
R_1 (F_0)^a	0.0330	0.0378	0.0641	0.0500
$wR_2(F_0^2)^a$	0.0866	0.0672	0.1572	0.0906
GOF	0.872	0.653	1.056	0.732

$^a R_1(F_0) = [(\sum||F_o| - |F_c||)/(\sum|F_0|)]$, and $wR_2(F_0^2) = [\sum[w(F_0^2 - F_c^2)^2]/\sum[w(F_0^2)^2]]^{1/2}$; where $w = 1/[\sigma^2(|F_0|) + (0.03P)^2]$, with $P = (F_0^2 + 2F_c^2)/3$.

another mononegative bridging ligand, in order to generate new (M−L₂−bpa) compounds (L = bridging ligand). With this aim in mind, we selected dca: a ligand that, similarly to azide, exhibits a great versatility in its coordination modes. Thus, besides the monodentate terminal coordination,[6] bidentate,[7] tridentate,[8] and even tetradentate[9] fashions have been reported for dca (Scheme 1). The potentiality of dca for the preparation of extended frameworks is illustrated by the great deal of attention focused on coordination polymers containing this ligand.[10,11]

Taking into account the above-mentioned aspects, four compounds of general formula [M(dca)₂(bpa)] [where M is the divalent transition cation: Mn (**1**), Fe (**2**), Co (**3**), and Zn (**4**)] have been synthesized and characterized structurally, spectroscopically, and magnetically. Compounds are isostructural and show a one dimensional (1D) structure, consisting of chains with the M(II) ions bridged by double $\mu_{1,5}$ dca ligands and unusually by a third bridge corresponding to the bpa ligand. Besides, a 3D interpenetrated compound of formula [Ni(dca)(bpa)₂]dca·6H₂O (**5**) has been obtained, using the same synthesis procedure, with single bpa and dca bridges.

Experimental Section

Materials. All solvents and starting materials for synthesis were purchased commercially and were used as received. M(II) nitrate hydrates (Aldrich), 1,2-bispyridylethane (Lancaster), and sodium dca (Aldrich) were used without further purification.

Synthesis of [Mn(dca)₂(bpa)]_n (1). This compound was synthesized by slow addition of a methanolic solution (15 mL) containing sodium dca (0.178 g, 2 mmol) and Mn(NO₃)₂·6H₂O (0.287 g, 1 mmol) to a solution of bpa ligand (0.158 g, 1 mmol) in the same solvent (5 mL). Yellow prismatic crystals appeared after two weeks from the resulting solution, which was left standing at room

(11) (a) Carranza, J.; Brennan, C.; Sletten, J.; Lloret, F.; Julve, M. *J. Chem. Soc., Dalton Trans.* **2002**, 3164–3170. (b) Dalai, S.; Mukherjee, P. S.; Zangrando, E.; Chaudhuri, N. R. *New J. Chem.* **2002**, *26*, 1185–1189. (c) Dalai, S.; Mukherjee, P. S.; Ribas, J.; Diaz, C.; Zangrando, E.; Chaudhuri, N. R. *Indian J. Chem., Sect. A: Inorg., Bio-inorg., Phys., Theor. Anal. Chem.* **2003**, *42*, 2250–2256. (d) Ghoshal, D.; Mostafa, G.; Maji, T. K.; Zangrando, E.; Lu, T.-H.; Ribas, J.; Chaudhuri, N. R. *New J. Chem.* **2004**, *28*, 1204–1213. (e) Maji, T. K.; Matsuda, R.; Kitagawa, S. *Nat. Mater.* **2007**, *6*, 142–148.

Table 2. Crystallographic Data and Processing Parameters for the Co Compound (**3**)^a

	Co (**3**)
formula	$CoC_{16}N_8$
M_r	363.17
cryst. syst.	monoclinic
space group	$C2/c$
a [Å]	16.612(2)
b [Å]	9.6246(13)
c [Å]	12.9957(17)
β [°]	123.319(4)
V [Å³]	1741.9(4)
Z	4
λ, [Å]	Cu K_α
R_b^a	3.3
R_p^b	4.8
R_{wp}^c	6.2
$N - P + C$	2250
χ^{2d}	2.54

$^a R_b^a = 100[\sum(I_{oi} - I_{ci})]/\sum(I_o; R_p^b = 100[\sum(y_{oi} - y_{ci})]/\sum(y_{oi}); R_{wp}^c = [M/\sum[w (y_{oi})^2]]^{1/2}; \chi^d = [M/N - P + C]^2; R_p$ and R_{wp} values are background uncorrected; $M = \sum[w (y_{oi} - y_{ci})^2]; N =$ number of data; $P =$ number of refined parameters; and $C =$ number of restrictions.

temperature. The crystals were filtered off, washed with ether, and dried in air. Yield of 42.3%. Anal. calcd for C₁₆H₁₂N₈Mn: C, 51.76; H, 3.26; N, 30.18. Found: C, 51.23; H, 3.12; N, 29.47.

Synthesis of [Fe(dca)₂(bpa)]_n (2). This compound was synthesized by the same method as **1** but using Fe(NO₃)₂·6H₂O (0.288 g, 1 mmol). Red-brown prismatic crystals appeared after one week from the resulting solution, which was left standing at room temperature. The crystals were filtered off, washed with ether, and dried in air. Yield of 62.2%. Anal. calcd for C₁₆H₁₂N₈Fe: C, 51.64; H, 3.25; N, 30.11. Found: C, 51.33; H, 3.07; N, 29.68.

Synthesis of [Co(dca)₂(bpa)]_n (3). This compound was synthesized by the same method as **1** but using Co(NO₃)₂·6H₂O (0.291 g, 1 mmol). Red prismatic crystals suitable for X-ray diffraction appeared after two weeks from the resulting solution, which was left standing at room temperature. The crystals were filtered off, washed with ether, and dried in air. Yield of 42.8%. Anal. calcd for C₁₆H₁₂N₈Co: C, 51.21; H, 3.22; N, 29.86. Found: C, 51.95; H, 3.27; N, 29.22.
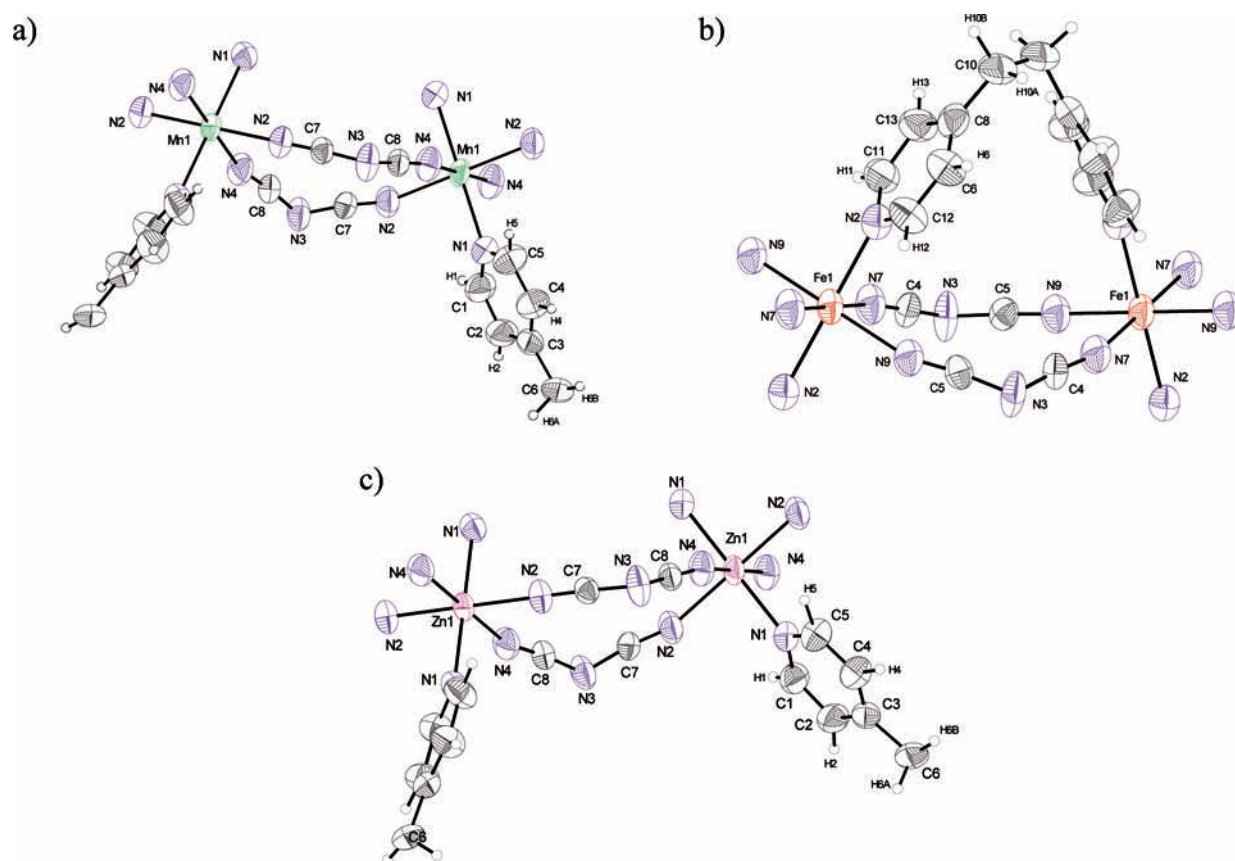
Synthesis of [Zn(dca)₂(bpa)]_n (4). This compound was synthesized by the same method as **1** but using Zn(NO₃)₂·6H₂O (0.297 g,

Table 3. Selected Bond Lengths (Å) and Angles (°) for Compounds Mn (**1**), Fe (**2**), and Zn (**4**)

[Mn(dca)₂bpa] (**1**)		[Fe(dca)₂bpa] (**2**)		[Zn(dca)₂bpa] (**4**)	
Mn(1)−N(1)	2.265(2)	Fe(1)−N(2)	2.190(3)	Zn(1)−N(1)	2.144(2)
Mn(1)−N(2)	2.224(2)	Fe(1)−N(9)	2.162(4)	Zn(1)−N(2)	2.167(2)
Mn(1)−N(4)^b	2.229(2)	Fe(1)−N(7)^b	2.155(4)	Zn(1)−N(4)^d	2.173(2)
N(1)−C(1)	1.322(3)	N(2)−C(11)	1.328(5)	N(1)−C(1)	1.330(3)
N(1)−C(5)	1.333(3)	N(2)−C(12)	1.329(5)	N(1)−C(5)	1.340(3)
N(2)−C(7)	1.144(3)	C(4)−N(7)	1.135(5)	N(2)−C(7)	1.139(3)
N(3)−C(7)	1.293(3)	N(3)−C(4)	1.301(5)	N(3)−C(7)	1.294(3)
N(3)−C(8)	1.300(3)	N(3)−C(5)	1.294(5)	N(3)−C(8)	1.304(3)
N(4)−C(8)	1.136(3)	C(5)−N(9)	1.142(5)	N(4)−C(8)	1.133(3)
N(1)^a−Mn(1)−N(1)	180.0	N(2)−Fe(1)−N(2)^h	180.0(1)	N(1)^d−Zn(1)−N(1)	180.0
N(2)−Mn(1)−N(2)^a	180.0	N(7)^b−Fe(1)−N(7)^g	180.0	N(2)^d−Zn(1)−N(2)	180.0
N(4)^b−Mn(1)−N(4)^c	180.0	N(9)^h−Fe(1)−N(9)	180.0	N(4)^e−Zn(1)−N(4)^f	180.0
N(2)^a−Mn(1)−N(1)	89.49(8)	N(7)^b−Fe(1)−N(2)	89.48(12)	N(1)−Zn(1)−N(2)	90.21(8)
N(4)^b−Mn(1)−N(1)	90.50(8)	N(9)−Fe(1)−N(2)	89.61(12)	N(1)−Zn(1)−N(4)^e	89.62(10)
N(2)−Mn(1)−N(4)^b	90.55(9)	N(7)^b−Fe(1)−N(9)	91.26(13)	N(2)−Zn(1)−N(4)^e	89.64(9)

^{a} −x − 1/2, −y + 1/2, −z + 1. ^{b} x + 1/2, −y + 1/2, z + 1/2. ^{c} −x − 1, y, −z + 1/2. ^{d} −x + 3/2, −y + 3/2, −z. ^{e} −x + 1, y, −z − 1/2. ^{f} x + 1/2, −y + 3/2, z + 1/2. ^{g} −x, y, −z + 1/2. ^{h} −x + 1/2, −y + 1/2, −z + 1.

Figure 1. Ortep view, 50% probability ellipsoids, with atom numbering scheme for: (a) compound **1**, (b) compound **2**, and (c) compound **4**.

1 mmol). Red prismatic crystals suitable for X-ray diffraction appeared after two weeks from the resulting solution, which was left standing at room temperature. The crystals were filtered off, washed with ether, and dried in air. Yield of 46.5%. Anal. calcd for C₁₆H₁₂N₈Zn: C, 50.35; H, 3.17; N, 29.36. Found: C, 50.85; H, 3.22; N, 28.75.

Synthesis of [Ni(dca)(bpa)₂]dca·6H₂O (5). This compound was synthesized by the same procedure as the other four; slow addition of a methanolic solution (15 mL) containing sodium dca (0.178 g, 2 mmol) and Ni(NO₃)₂·6H₂O (0.291 g, 1 mmol) to a solution of bpa ligand (0.158 g, 1 mmol) in the same solvent (5 mL). However, an immediate blue precipitate appearing was dissolved again. Blue prismatic crystals of this compound appeared after two weeks from the resulting solution, which was left

standing at room temperature. The crystals were filtered off, washed with ether, and dried in air. Yield of 26.5%. Anal. calcd for C₂₈H₃₆N₁₀O₆Ni: C, 50.39; H, 5.44; N, 20.99. Found: C, 50.59; H, 5.32; N, 21.88.

Physical Techniques. Microanalyses were performed with a LECO CHNS-932 analyzer. Infrared spectroscopy was performed on a MATTSON FTIR 1000 spectrophotometer as KBr pellets in the 400−4000 cm⁻¹ region. Diffuse reflectance spectra were registered at room temperature on a CARY 2415 spectrometer in the range 5000−45 000 cm⁻¹. Electron spin resonance (ESR) spectroscopy was performed on powdered samples at the X-band frequency, with a Bruker ESR 300 spectrometer equipped with a standard OXFORD low-temperature device, which was calibrated by the NMR probe for the magnetic field. The frequency
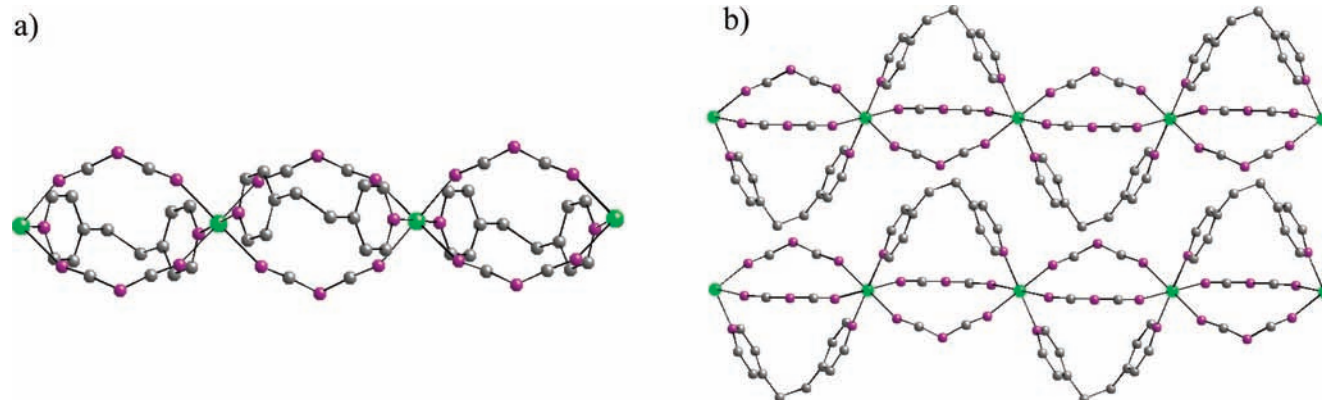
Figure 2. (a) View [101] of the chain M−(dca)$_2$bpa−M, and (b) packing of the chains along the direction [010].
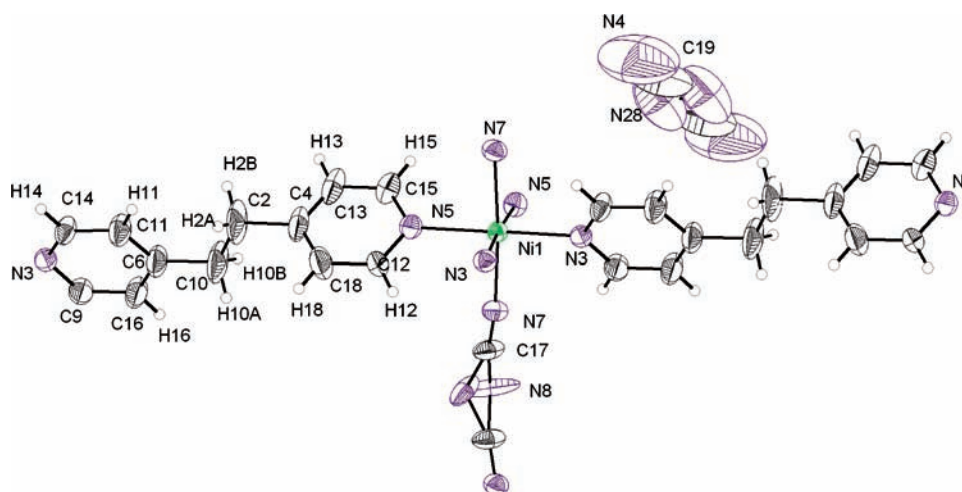

Figure 3. Ortep view with atom numbering scheme showing 50% probability ellipsoids of compound **5** (water molecules have been omitted for clarity).

was measured with a Hewlett-Packard 5352B microwave frequency computer. The magnetic susceptibilities of polycrystalline samples of the complexes were carried out in the temperature range 2−300 or 4−300 K at a value of the magnetic field of 1000 G, using a Quantum Design Squid susceptometer equipped with a helium continuous-flow cryostat. The complex (NH$_4$)Mn(SO$_4$)$_2$·6H$_2$O was used as a susceptibility standard. The experimental susceptibilities were corrected for the diamagnetism of the constituent atoms (Pascal tables).[12]

Crystal Structure Determination. Single crystals of compounds **1** and **4** were glued to a thin glass fiber with epoxi resin and collected, at room temperature, on an Enraf-Nonius CAD-4 automatic four-circle diffractometer with graphite-monochromated Mo K$_\alpha$ radiation ($\lambda = 0.71070$ Å), operating in $\omega/2\theta$ scanning mode using suitable crystals for data collection. Accurate lattice parameters were determined from least-squares refinement of 25 well-centered reflections. Intensity data were collected in the θ range 2.65−25.77° for the compound **1** and in the θ range 2.57−29.99°for the compound **4**. Single crystals of compounds **2** and **5** were glued to a thin glass fiber and collected, at room temperature, on an STOE IPDS I (imaging plate diffraction system) diffractometer with graphite-monochromated Mo K$_\alpha$ radiation ($\lambda = 0.71070$ Å). Accurate lattice parameters were determined from 1213 and 1713 reflections for compounds **2** and **5**, respectively. Intensity data were collected in the θ range 2.57−25.87° for compound **2** and 2.06−26.00° for compound **5**. Corrections for Lorentz and polariza-

Table 4. Selected Bond Lengths (Å) and Angles (°) for Compound **5**

Ni−N(3)	2.101(4)	N(3)−Ni−N(7)	91.93(16)
Ni−N(5)	2.155(4)	N(5)^a−Ni−N(7)^a	86.88(15)
Ni−N(7)	2.079(4)	N(5)^a−Ni−N(7)	88.14(16)
N(3)^a−Ni−N(3)	86.4(2)	N(7)−Ni−N(7)^a	172.8(3)
N(3)−Ni−N(5)	176.52(18)	N(3)−Ni−N(5)^a	90.42(13)
N(5)−Ni−N(5)^a	92.8(2)	C(17)−N(7)−Ni	168.5(4)
N(3)−Ni−N(7)^a	93.34(16)		

^{a} −x, y, −z + 3/2.

tion factors were applied to the intensity values. The structure was solved by direct methods using the program SIR97[13] and refined by a full-matrix least-squares procedure on F^2 using SHELXS97.[14] Nonhydrogen atomic scattering factors were taken from the International Tables of X-ray Crystallography.[15a] In Table 1, crystallographic data and processing parameters for compounds **1**, **2**, **4**, and **5** are shown. An isomorphous to compound **1** has been reported.[11b]

(12) Earnshaw, A. *Introduction to Magnetochemistry*; Academic Press: London, 1968.

(13) Altomare, A.; Burla, M. C.; Camalli, M.; Cascarano, G. L.; Giacovazzo, C.; Guagliardi, A.; Moliterni, A. G. G.; Polidori, G.; Spagna, R. *J. Appl. Crystallogr.* **1999**, *32*, 115–119.

(14) Sheldrick, G. M. *Acta Crystallogr.* **2008**, *A64*, 112–122.

(15) (a) Cromer, D. T.; Waber, J. T. *International Tables for X-Ray Crystallography*, Vol. *IV*, Kynoch Press: Birmingham, U.K., 1974. (b) Rodriguez-Carvajal, J. *FULLPROF: A Program for Rietveld Refinement and Pattern Matching Analysis*; Abstracts of the Satellite Meeting on Powder Diffraction of the XV Congress of the IUCr; Toulouse, France, 1990, p 127. (c) Rietveld, H. M. *Acta Crystallogr.* **1967**, *12*, 151–152. (d) Rietveld, H. M. *J. Appl. Crystallogr.* **1969**, *6*, 65–67.
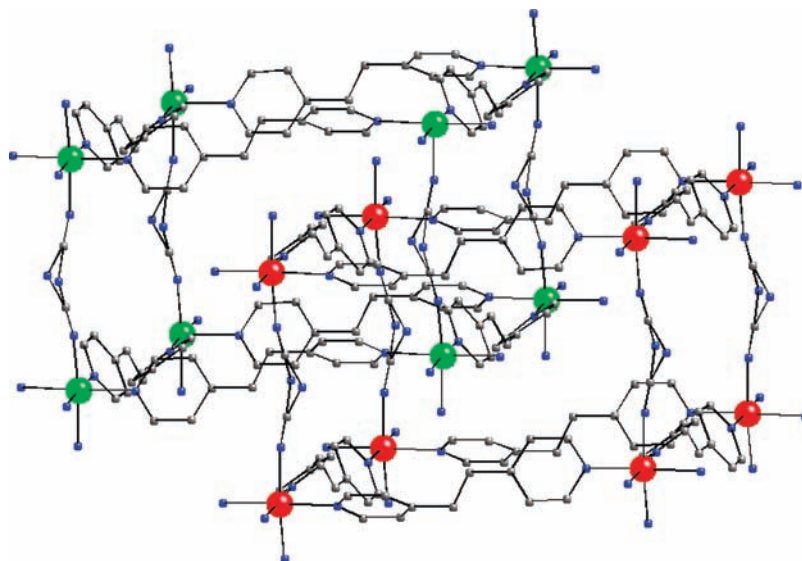
Figure 4. View of the interpenetration of the two 3D grids.

Table 5. Selected Most Important Intermolecular Hydrogen Bonds for Compound **5**

O1w−H1O1	O1w⋯N4	H1O1⋯N4	O1w−H1O1⋯N4
0.85(14)	2.40(3)	1.8(2)	132(16)
O1w−H2O1	O1w⋯O2w	H2O1⋯O2w	O1w−H2O1⋯O2w
0.84(19)	2.07(4)	1.54(7)	117(13)
O2w−H1O2[a]	O2w⋯O3w	H1O2⋯O3w	O2w−H1O2⋯O3w
0.87(8)	2.38(4)	1.72(8)	130(6)
O2w−H2O2[a]	O2w⋯O3w	H2O2⋯O3w	O2w−H2O2⋯O3w
0.87(8)	3.01(4)	2.29(7)	140(7)

[a] $-x, y, -z + 3/2$.

X-ray powder diffraction data for compound **3** were collected on a PHILIPS X'PERT powder diffractometer with Cu K$_\alpha$ radiation in steps of 0.03° (2θ) over the 7.01−69.99° (2θ) angular range and a fixed-time counting of 4 s at 25 °C. X-ray diffraction patterns for Co (**3**) were refined, with the FULLPROF[15b] program based on the Rietveld method,[15c,d] by using as initial values the cell parameters, space group, and atomic coordinates of compound Mn (**1**). The experimental, calculated (according to the best-fit parameters shown in Table 2), and difference patterns can be observed in Figure S1, Supporting Information. These results confirm the isostructural character of compounds (**1**−**4**) (see Table 2).

Results and Discussion

Structural Analysis. The four compounds **1**−**4** are isostructural, exhibiting some slight differences in structural parameters. Selected bond distances and angles are collected in Table 3, and perspective views of the structures Mn (**1**), Fe (**2**), and Zn (**4**) are depicted in Figures 1 and 2.

The structures consist of uniform chains in which adjacent metal ions are triple linked by two dca and one bpa bridge. Every metal ion is coordinated to two pyridyl nitrogen from bpa ligands (at the axial sites) and four nitrile nitrogen from dca (at equatorial positions) (Figure 1). The M−N$_{bpa}$ distance [2.265(2), 2.190(3), 2.144(2) Å for compounds **1**, **2**, and **4**, respectively] is slightly larger than that of M−N$_{dca}$ [2.224(2), 2.159(5), and 2.167(2) Å for compounds **1**, **2**, and **4**, respectively] for the Mn (**1**) and Fe

(16) Miller, J. N.; Miller, J. C. *Statics and Chemometrics for analytical Chemistry*, 4th ed.; Pearson Education Limited: England, 2000.
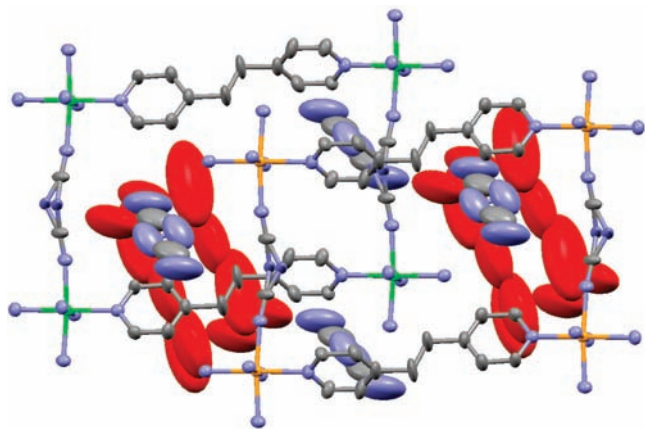
(**2**) that show slightly elongated octahedron polyhedra but not for the Zn (**4**) showing a slightly compressed octahedron polyhedron.[16] In compound **4**, the distances and the angles are slightly lower due to the contraction of the completely filled d orbital.

In these unusual triple-bridged chains, the bpa ligands adopt the gauche conformation with a very low torsion angle (47, 47.9, and 49° for compounds **1**, **2**, and **4**, respectively) to accommodate to the M−(dca)$_2$−M separation. In the present complexes, the M(dca)$_2$ chains are bent into an unusual boat conformation, yielding a sinusoidal chain. Obviously, the distortion of these chains from linear to sinusoidal is induced by the gauche coordination of the bpa ligand. On the other hand, due to the extremely high flexibility of bpa, this ligand can adopt a noticeable low py−C−C−py angle to get accommodated to the M⋯M distances, (7.3 for compound **1** and 7.2 Å for compounds **2** and **4**) imposed by the dca ligands. These chains extend along the [101] direction (Figure 2a). On the other hand, Figure 3b shows the bpa ligands adopting the gauche conformation and forming arcs that are alternatively disposed upward and downward in relation to the dca ligands.

Views of the structures in the (001) plane are represented in Figure S2, Supporting Information, where it can be observed as two different pseudochannels. The first consisting of the dca ligands and the latter by the arches of the bpa.

The structure of [Ni(dca)(bpa)$_2$]dca·6H$_2$O (**5**) consists of two-fold interpenetrated α-Po-like (simple cubic phase) networks. The coordination environment of the Ni (II) ion, with atom numbering, is shown in Figure 3. Four bpa groups occupy the equatorial positions of the coordinating sphere [Ni(1)−N(3)$_{bpa}$ = 2.101(4) Å and Ni(1)−N(5)$_{bpa}$ = 2.155(4) Å], whereas the axial ones are occupied by two N-bonded dca ligands [Ni(1)−N$_{dca}$ = 2.079(4) Å] (Table 4), conforming a compressed octahedron polyhedron.

Each bpa ligand, in anti conformation, acts as a bridge coordinating to two nickel atoms via the two extreme 4,4′ nitrogen atoms. These bpa ligands connect the Ni(II) atoms into square grid-like [Ni(bpa)$_2$]$_n$ sheets (x,y plane), while these sheets are further connected to each other

Figure 5. View of the disposition of the free dca and solvent molecules (red) in the voids. Both showing large thermal parameters.

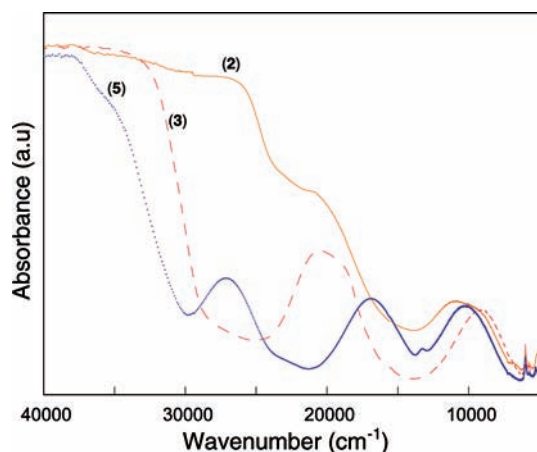**Figure 6.** UV−vis spectra of compounds **2**, **3**, and **5**.

Table 6. IR Bands (cm^{-1}) and Assignments for Compounds **1**−**5**

compound bands[18]	(1)	(2)	(3)	(4)	(5)
$\nu_{assym+sym}(C\equiv N)$	2300	2307	2305	2300	2315
$\nu_{assym}(C\equiv N)$	2230	2240	2237	2245	2260
$\nu_{sym}(C\equiv N)$	2175	2180	2180	2175	2195
$\nu(C=C,C=N)$	1615	1615	1600	1615	1605
$\nu(C-C,C-N)$	1360	1355	1350	1360	1385
$\nu(C-H)$	825/810	820/810	835/810	830/810	840/815
$\nu(M-N)$	535/515	535/520	540/520	535/520	550/505

Table 7. UV−Vis Bands (cm^{-1}) and Assignments for Compounds **2**, **3**, and **5**

compound	transition	band	ν (cm^{-1})
(2)	$^5T_{2g} \rightarrow {}^5A_1$	ν_{1A}	9200
	$^5T_{2g} \rightarrow {}^5B_1$	ν_{1B}	11 000
(3)	$^4T_{1g}(F) \rightarrow {}^4T_{2g}$	ν_1	9200
	$^4T_{1g}(F) \rightarrow {}^4A_{2g}$	ν_2	19 000
	$^4T_{1g}(F) \rightarrow {}^4T_{1g}(P)$	ν_3	20 500
(5)	$^3A_{2g} \rightarrow {}^3T_{2g}$	ν_1	10 200
	$^3A_{2g} \rightarrow {}^1E_g$	$\nu_2{}^a$	13 350
	$^3A_{2g} \rightarrow {}^3T_{1g}(F)$	ν_3	16 500
	$^3A_{2g} \rightarrow {}^3T_{1g}(P)$	ν_4	27 000

^{a}Spin-forbidden transition.

In spite of the interpenetration, there are large voids in the global structure that are occupied by the free dca ligand (counterion) and the crystallization water molecules showing hydrogen bonding (see Table 5). These molecules are responsible for the interpenetration of the grids not to be centered, but displaced each other (see Figure 5).

Infrared Spectra. The most important aspects concerning the infrared spectra of compounds **1**−**5** deal with the possibility of characterizing the presence of the different coordination modes of the bpa and dca ligands.

The IR spectra of the five compounds are quite similar and exhibit three strong absorptions in the 2300−2170 cm^{-1} region characteristic of the dca ligand. The bands at about 2175, 2180, 2180, 2195, and 2175 cm^{-1} (very strong) for **1**−**5**, respectively, correspond to symmetric $\nu_{C\equiv N}$ mode of this ligand. The characteristic bands of the pyridyl rings in the bpa are shown around 1600 and 1350 cm^{-1} in all the five compounds (Figure S4, Supporting Information, and Table 6).

UV−vis Spectroscopy. The diffuse reflectance spectra for compounds **2**, **3**, and **5** can be observed in Figure 6, and the results have been shown in the Table 7. The spectra have been interpreted following Tanabe−Sugano diagrams.[19] The results are in good agreement with the values found in the literature for each ion in their coordination environment.[20]

The diffuse reflectance spectrum for compound **2** exhibits a single allowed transition ($^5T_{2g} \rightarrow {}^5E_g$) split due to the Jahn−Teller effect (^5E_g is split into $^5A_1 + {}^5B_1$). At high wavenumbers, the spectrum shows a charge-transfer band overlapping with the triplet states. The values of Dq and the $(8/3)d\sigma$ are 920 and 1800 cm^{-1}, respectively.

in the [001] direction by the bridging dca to give a 3D network. (Figures 4 and S3, Supporting Information).

Large cavities are formed owing to the combination of the long distance between the Ni atoms and the ligand sizes; these cavities are able to accommodate another interpenetrating lattice (Figure 4). This phenomenon is also observed in the complexes M[N(CN)$_2$]$_2$(pyz),[17] where M = Mn (II), Fe (II), Co (II), Ni (II), and Zn (II) and pyz = pyrazine). The intranetwork Ni···Ni separations are 13.551 and 8.657 Å (through the bpa and dca ligand), these exceed the shortest Ni···Ni internetwork separation of 8.301 Å. The dca ligand possesses pseudo-C_{2v} symmetry with C≡N bond distances ranging from 1.135 to 1.147 Å. The central amide nitrogen in the N(CN)$_2^-$ ligand was positionally disordered owing to the relatively large cavities in the system and the hydrogen bonding (Table 5). The structure is completed with another N(CN)$_2^-$ ion acting as a counterion and six water crystallization molecules that site in the voids of the interpenetrating structure showing large thermal parameters (Figure 5).

(17) (a) Manso, J. L.; Incarvito, C. D.; Rheingold, A. L.; Miller, J. S. *J. Chem. Soc., Dalton Trans.* **1998**, 3705–3706. (b) Jensen, P.; Batten, S. R.; Fallon, G. D.; Hockless, D. C. R.; Moubaraki, B.; K. S. Murray, K. S.; Robson, R. *J. Solid State Chem.* **1999**, *145*, 387–393. (c) Jensen, P.; Batten, S. R.; Moubaraki, B.; Murray, K. S. *J. Solid State Chem.* **2001**, *159*, 352–361. (d) Brown, C. M.; Manson, J. L. *J. Am. Chem. Soc.* **2002**, *124*, 12600–12605.

(18) (a) Nakamoto, K. *Infrared Spectra of Inorganic and Coordination Compounds*, 5th ed.;John Wiley & Sons: Hoboken, NJ, 1997; (b) Pretsch, E.; Clerc, T.; Seibl, J.; Simon, W. *Tablas para la Elucidación Estructural de Compuestos Orgánicos por Métodos Espectroscópicos*; Alhambra: Barcelona, 1980.

(19) Tanabe, Y.; Sugano, S. *J. Phys. Soc. Jpn.* **1954**, *9*, 753.

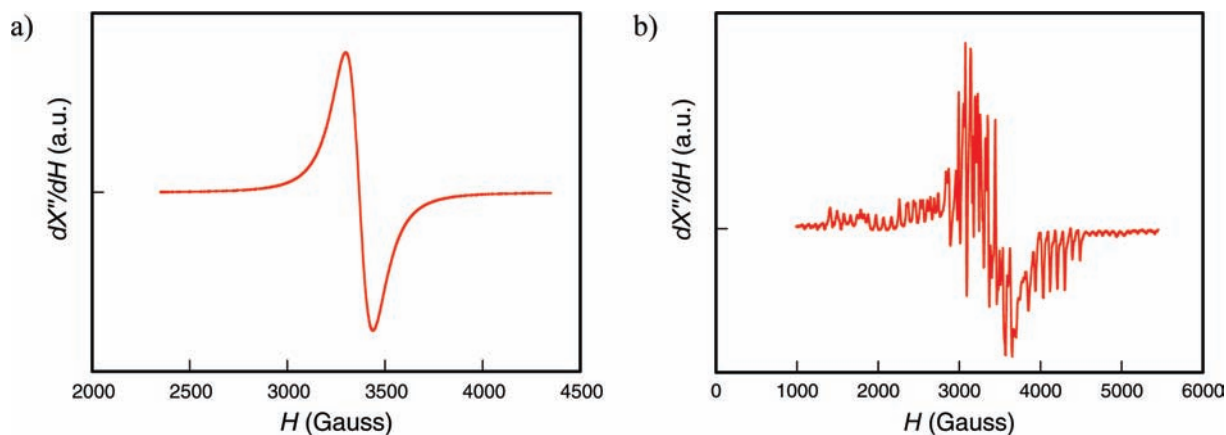(20) Lever, A. B. P. *Inorganic Electronic Spectroscopy*; Elsevier: London, 1984.

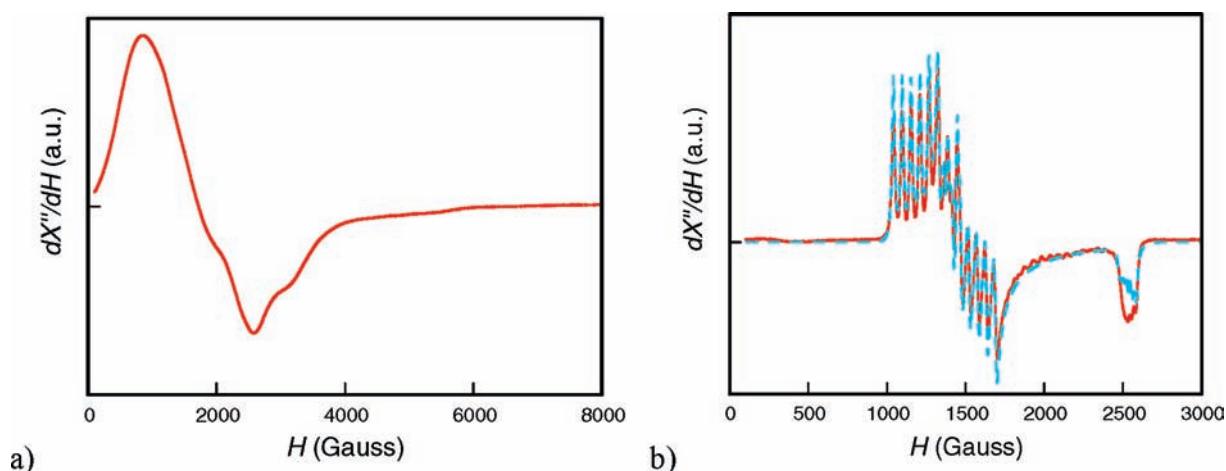**Figure 7.** X-band powdered EPR spectra at room temperature of: (a) complex **1** and (b) Mn-doped [$Zn_{0.95}Mn_{0.05}(dca)_2bpa$] system.

Figure 8. X-band powdered EPR spectra of: (a) compound **3** at $T = 20$ K and (b) Co-doped [$Zn_{0.997}Co_{0.003}(dca)_2bpa$] at $T = 4$ K. The solid line shows the observed spectra, and the discontinuous line shows the calculated spectra.

The diffuse reflectance spectrum for compound **3** exhibits three transitions attributed to spin-allowed transitions from $^4T_{1g} \rightarrow ^4T_{2g}$, $^4A_{2g}$, and $^4T_{1\ g}$, as corresponds to high-spin octahedral Co^{II}. At 35 000 cm^{-1} the spectrum shows a charge-transfer band. The values calculated from these transitions are $Dq = 980$ and $B = 870$ cm^{-1}. The value of B is indicative of an 89.6% of covalence of the Co–N bonds in this compound.

For **5**, the UV–vis spectrum exhibits the typical transitions for octahedral Ni(II) compounds[19,20] with values of $Dq = 1020$, $B = 880$ (84.5% covalence), and $C = 3382$ cm^{-1} ($C/B = 3.84$) calculated for spin-allowed transitions from $^3A_{2g} \rightarrow ^3T_{2g}$, $^3T_{1g}(F)$, $^3T_{1\ g}(P)$ and the spin-forbidden transition from $^3A_{2g} \rightarrow ^1E_g$.

EPR Spectroscopy and Magnetic Properties. X-band powdered electron paramagnetic resonance (EPR) spectra for compounds **1** and **3** were recorded at room temperature down to 4.2 K. Besides, due to the isomorphism with the Zn compound (**4**), X-band EPR spectra of Mn- and Co-doped [$Zn_{0.95}Mn_{0.05}(dca)_2bpa$] and [$Zn_{0.997}Co_{0.003}(dca)_2bpa$] compounds have been recorded. This is in order to study the behavior of the different ions in diluted systems.

Figure 7a shows the room temperature EPR spectrum of compound **1**. As can be observed, an isotropic signal appears centered at a g_{iso} value of 2.002. This signal is characteristic of the Mn(II) ion in an octahedral environment.

As can be observed (Figure 7b), the number of signals is greater than the corresponding 6 signals expected for the hyperfine coupling. This could be indicative of the presence of a significant zero field splitting. The great number of signals observed does not let us make calculations in order to obtain the hyperfine coupling constant.

In the case of compound **3**, Figure 8a shows the EPR spectrum at 20 K. The low-temperature EPR spectra for Co(II) ions ($S = 1/2$) usually shows a very wide signal with a **g** tensor next to the isotropic and with values in the order of 4.33. In this case, due to the high wideness of the signal, calculations of accurate values of the **g** tensor have not been possible.

A rhombic symmetry of the **g** tensor can clearly be observed, together with the hyperfine coupling constant (Figure 8b). The simulation of the EPR spectrum, discontinuous line in Figure 8b, gave us the following set of values: $\mathbf{g}_1 = 5.43$, $A_1 = 147 \times 10^{-4}$; $\mathbf{g}_2 = 4.475$, $A_2 = 109 \times 10^{-4}$; and $\mathbf{g}_3 = 2.665$, $A_3 = 20 \times 10^{-4}$. These values are in good agreement with those observed for Co(II) ions in an octahedral environment with a rhombic symmetry.

The magnetic susceptibilities of the Mn (**1**), Fe (**2**), and Co (**3**) compounds were measured in the 4.2–300 K temperature range and showed that χ_m values continuously increase upon cooling for the three compounds, not exhibiting any maxima in the whole studied temperature range.
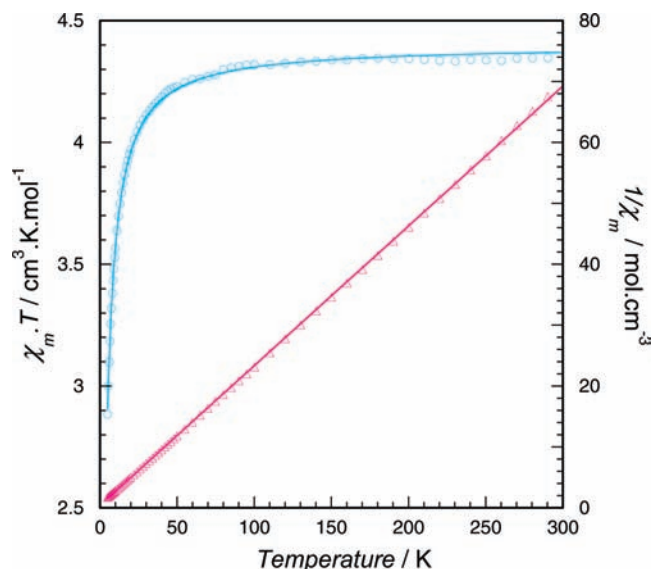
Figure 9. Thermal evolution of $\chi_m T$ and χ_m^{-1} for compound **1** and the corresponding theoretical Curie−Weiss law. The solid curve showing the best fit of experimental data to eq 1.

Figure 10. Thermal evolution of $\chi_m T$ and χ_m^{-1} for compound **2** and the corresponding theoretical Curie−Weiss law. The solid curve showing the best fit obtained by eq 2.

Figure 9 shows the thermal variation of the reciprocal magnetic susceptibility, χ_m^{-1}, and the $\chi_m T$ product for **1**. The $\chi_m T$ magnitude continuously decreases upon cooling. On the other hand, χ_m^{-1} has been observed to follow the Curie−Weiss law over the measured temperature range with $C_m = 4.36$ cm³ K mol⁻¹ and $\theta = -0.09$ K.

These data suggest the presence of weak antiferromagnetic interactions taking place through the triple Mn−(dca)₂bpa−Mn bridges. In order to evaluate the exchange constant, we have used the analytical expression[21] for an infinite chain of classical spins, scaled to $S = 5/2$ (eq 1), derived by Fisher and based upon the spin Hamiltonian $H = -2J\sum S_i S_{i+1}$

$$\chi_m = \frac{Ng^2\beta^2 S(S+1)}{3kT}\left(\frac{1-u}{1+u}\right);$$

$$\text{where } u = \frac{T}{T_o} - \coth\frac{T}{T_o}; \quad T_o = \frac{2JS(S+1)}{k} \quad (1)$$

where N and k are the Avogadro and Boltzmann constants, respectively, g is the Landé factor, and β is the Bohr magneton. According to eq 1, the best-fit parameters for compound **1** have been determined to be $g = 2.00$ and $J/k = -1.8$ K.

The experimental data for compound **2**, plotted as the thermal variation of the reciprocal susceptibility and the $\chi_m T$ product are shown in Figure 10. The variation of χ_m^{-1} is well described by the Curie−Weiss law within the whole range of temperature, with values of C_m and θ of 3.39 cm³ K mol⁻¹ and −0.59 K, respectively. The $\chi_m T$ term is practically constant down to 100 K, rapidly decreasing upon further cooling.

The thermal variation of $\chi_m T$ together with the sign of the Weiss constant is consistent with the occurrence of antiferromagnetic couplings. eq 2 can be proposed as a theoretical approach to the magnetic behavior of com-
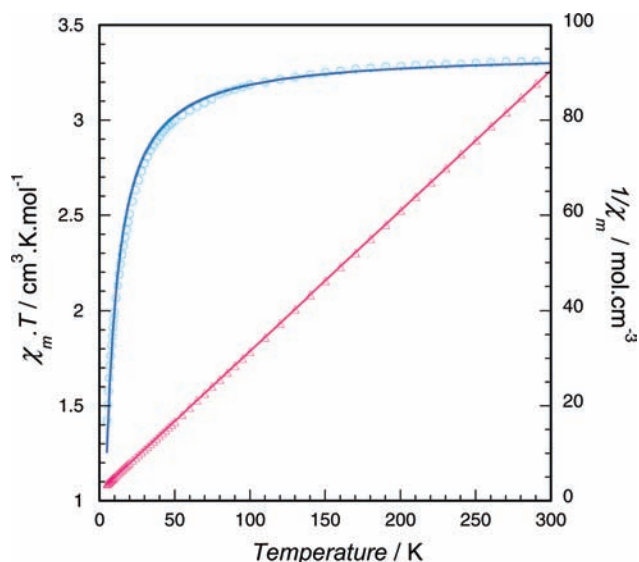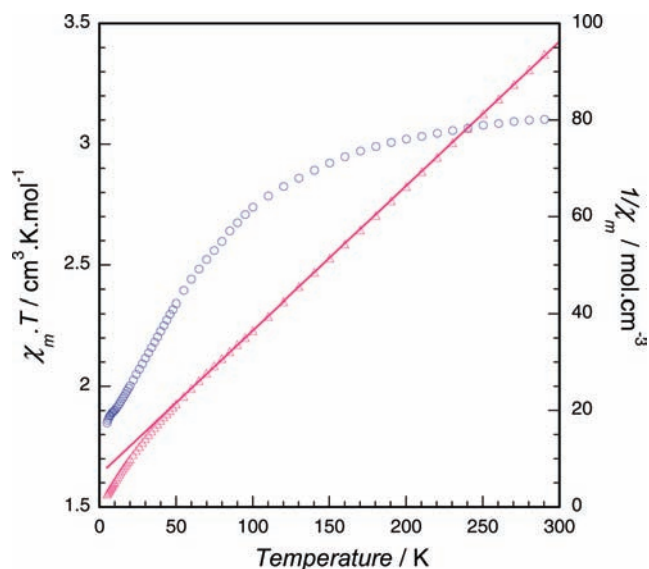

Figure 11. Thermal evolution of $\chi_m T$ and χ_m^{-1} for compound **3** and the corresponding theoretical Curie−Weiss law (solid line).

pound **2**. In this expression, χ_m is a function of the J parameter due to exchange couplings along an infinitive-spin linear chain[21] with $S = 2$:

$$\chi_m = \frac{6Ng^2\beta^2}{3kT}\left[\frac{1-u}{1+u}\right];$$

$$\text{where } u = \frac{T}{T_o} - \coth\left(\frac{T}{T_o}\right) \text{ and } T_o = 12\frac{J}{K} \quad (2)$$

According to eq 2, the best-fit parameters for compound **2** have been determined to be $g = 2.11$ and $J/k = -0.66$ K. The value of g lies among the usual ones for octahedral Fe(II) ions (2.08−2.33).[22]

(21) Fisher, M. E. *Am. J. Phys.* **1964**, *32*, 343.

(22) Mabbs, F. E.; Machin, D. J. *Magnetism and Transition Metal Complexes*; Chapman and Hall: London, 1973.
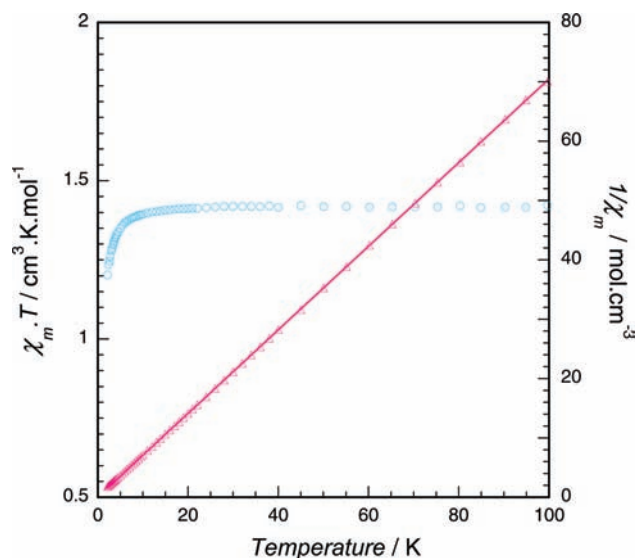
Figure 12. Thermal evolution of $\chi_m T$ and χ_m^{-1} for compound **5** and the corresponding theoretical Curie–Weiss law (solid line).

Plots of χ_m^{-1} and $\chi_m T$ vs temperature are shown in Figure 11 for compound **3**. As can be seen, the Curie–Weiss law is followed at temperatures down to 50 K, with values of C_m and θ of 3.49 cm^3 K mol^{-1} and −1.99 K, respectively. The decreasing values of $\chi_m T$ upon cooling could be indicative the existence of antiferromagnetic couplings, as for the rest of the isomorphous compounds. However, the experimental value per Co at room temperature is 3.10 cm^3 K mol^{-1}, significantly larger than the spin-only value of high-spin cobalt(II) (1.88 cm^3 K mol^{-1}, $S = 3/2$) but slightly smaller than the value expected for the free ion in ^4F state with negligible spin–orbital coupling (3.38 cm^3 K mol^{-1}). This indicates a significant contribution of the orbital angular momentum, typical of the $^4T_{1g}$ ground term for Co(II) in an octahedral field. Thus, the decrease of μ_{eff} should be mainly attributed to the spin–orbital coupling together with weak intrachain antiferromagnetic interactions due to the dca bridges. The lack of an appropriate magnetic model to describe this situation has precluded quantitative magnetic analysis for this compound.

The experimental data for compound **5**, plotted as the thermal variation of the reciprocal susceptibility and the $\chi_m T$ product, are shown in Figure 12. The variation of χ_m^{-1} is well described by the Curie–Weiss law within the whole range of temperature, with values of C_m and θ of 1.42 cm^3

K mol^{-1} and −0.1 K, respectively. The $\chi_m T$ term is practically constant down to 50 K, very slowly decreasing upon further cooling. Both, the thermal variation of $\chi_m T$ together with the sign of the Weiss constant is consistent with the occurrence of slight antiferromagnetic coupling in the compound. Attempts to fit the magnetic data for this compound to a linear chain model (Ni−dca chains, $S = 1$) with a J' in the molecular field approximation (Ni−bpa bridges) have been unsuccessful. This may be due to the extreme weakness of the interactions observed or to requiring a specific model not yet available.

Conclusions

The combined use of dicyanamide (dca) and 1,2-bis(4-pyridyl)ethane (bpa) has led to the preparation of five extended frameworks with Mn(II), Fe(II), Co(II), Zn(II), and Ni(II) ions. The same type of unusual structural array has been obtained in four first cases: one-dimensional (1D) [M(dca)$_2$-(bpa)] (**1**−**4**) compounds with the metal(II) ions bridged by double $\mu_{1,5}$ dca ligands and unusually by a third bridge consisting of the bpa ligand, which shows one of the lowest torsion angles known to date. While in general M(dca)$_2$ is octahedral, Zn(dca)$_2$ is not, and therefore, it is to be noted that in this case compound **4** is octahedral. On the contrary, compound **5** shows a 3D structure of the α-Po like type with planes of Ni-bpa joined by dca ligands. Furthermore, two grids are interpenetrated in the global 3D structure. The relatively weak antiferromagnetic interactions are in agreement with the existence of double $\mu_{1,5}$-dca−single bpa bridges in compounds **1**−**3**. Lower antiferromagnetic interactions in compound **5** may be in agreement with the existence of only one dca bridge joining Ni(II) ions in this compound.

Supporting Information Available: Crystallographic information, as CIF files, for **1**, **2**, **4**, and **5** compounds. X-ray diffraction pattern for **3**, complementary structural figures, and IR spectra for all compounds. This material is available free of charge via the Internet at http://pubs.acs.org.